High frequency contactless characterization of 2D materials. Graphene, WS_2

David Arcos Dani Nuño Maria C. Santos Lluís Ametller Núria Ferrer-Anglada

D. Arcos, Dr. L. Ametller, Dr. N. Ferrer-Anglada
Department of Physics
Universitat Politècnica de Catalunya (UPC) Campus Nord, Barcelona, Spain
E-mail: nuria.ferrer@upc.edu
D. Nuño, Dr. M. C. Santos
TSC Department
Universitat Politècnica de Catalunya (UPC) Campus Nord, Barcelona, Spain

Keywords: *Graphene, WS_2, high frequency conductivity, terahertz, 2D material*

The electrical conductivity of two-dimensional materials without any electrical contact can be obtained using two different methods: the terahertz time domain spectroscopy (THz-TDS) method, in the range from GHz up to 2 THz [1], and with a rutile dielectric resonator (RDR), in which case the conductivity is obtained at the resonant frequency of the device, close to 9.0 GHz [2]. In one case (THz-TDS in a transmission setup), we focus directly on the sample. In the other case (RDR), the sample is placed inside the resonant cavity working at TE_{011} mode and must have exactly the same surface size as the cavity, 12×12 mm in our device. From the Q factor variation of the resonant cavity due to the sample, we can extract its surface resistance. We performed these measurements on different two-dimensional materials: graphene and WS_2. We analyzed and compared both methods.

1 Introduction

The measurement and characterization of two-dimensional (2D) materials such as graphene, molybdenum disulfide (MoS_2) or tungsten disulfide (WS_2), among others, is an active research field due to the particular electrical, chemical, thermal and mechanical properties that these materials show specially at high frequencies. There are a lot of applications of these crystalline single-layer materials: gas sensors [3], high-performance energy storage [4] and communication devices at the microwave, mid-IR and THz range of frequencies [5, 6].
WS_2 is an example of a transition metal dichalcogenide (TMDC) which, similar to graphite, is a layered material enabling the exfoliation into 2D layers of single unit cell thickness, due to its strong in-plane bonding and weak out-of-plane interactions [7]. WS_2 has an electronic gap between 1.4 eV (indirect) to 2 eV (direct) depending on its thickness (bulk, few layers or single layer). As it is well known, a direct gap is a desired characteristic for new devices applications in nanoelectronics and optoelectronics.
Terahertz time domain spectroscopy (THz-TDS) is a measuring technique based on a coherent detection very adequate for 2D materials characterization as no electrical contacts are nedded, in the range from some GHz up to 2 THz, we used it previously on MoS_2 and graphene [1]. Dielectric resonators are devices used for the characterization of surface electrical resistance of conducting coatings at frequencies around 10 GHz [2].
In this work, our main goal is to compare the THz-TDS and the dielectric resonator techniques for the electronic characterization of WS_2 and graphene at the microwave and THz range of frequencies.

1.1 Sample characterization

WS_2 samples were obtained by chemical vapor deposition (CVD) on quartz of 1 mm thickness at Sejong University, Seul, Korea (prof. J. Eom group). Graphene samples Gr-PET and Gr-Quartz were obtained (at Graphenea) by CVD on different substrates: Gr-PET is CVD on polyethylene terephthalate (PET) of 250 μm thickness and Gr-Quartz is CVD on quartz of 500 μm thickness. GrO and Gr-flakes are films of compacted graphene flakes of a few μm thickness from Danubia Nano Tech Ltd, GrO is a film of graphene oxide flakes and Gr-flakes is a film of graphene flakes after reducing a GrO film. The dimensions and notation for all the analyzed samples are shown on **Table 1**.

1.1.1 IR characterization

A Fourier-transform infrared absorbance spectroscopy (FT-IR) was done for WS_2 and graphene samples in the range from 4 000 to 6 000 cm^{-1} in order to check the optical behavior in the adjacent upper frequency range (see **Figure 1**). This analysis included the absorbance measurement of the quartz bare substrates to be used as a reference for each 2D material. The absorbance obtained for graphene samples was constant throughout the measurement range and very low (less than 1.5 %). In the case of WS_2 samples, the absorbance presented a linear behavior (increasing slightly with the wave number) and a higher value (between 25 % at 4 000 cm^{-1} and 30 % at 6 000 cm^{-1}). These results are in good agreement with the behavior at the visible range ($\sim$ 14 000 - 25 000 cm^{-1}), the WS_2 layer is clearly visible with the naked eye in comparison to the bare substrate, whereas in the case of graphene, the bare substrate and the sample are indistinguishable. Spectra were obtained with the Frontier FT-IR/FIR Spectrometer from Perkin Elmer at CCiTUB.

1.1.2 Raman characterization

The quality of the 2D samples were obtained by a Raman spectroscopy with an excitation laser line of 532 nm, with a power of 0.5 mW to ensure non-degradation of the samples, at CCiTUB.
Raman spectra of WS_2 on quartz samples show two main characteristic bands at 352 cm^{-1} and 418 cm^{-1}. E^1_{2g} and A_{1g} are the most significant active modes of the WS_2 Raman spectra [8] and, since the longitudinal acoustic phonon mode (2LA) is so close to the E^1_{2g} band (less than $\sim$ 5 cm^{-1} difference), a multi-peak Lorentzian fitting is needed (see **Figure 2**). After a deconvolution and baseline correction, the most prominent peak was decomposed into three lines: E^1_{2g} (M) line at 343 cm^{-1} with a relative intensity of 1.01 (a.u.), 2LA(M) line at 351 cm^{-1} with a relative intensity of 2.61 (a.u.) and $E^1_{2g}(\Gamma)$ line at 355 cm^{-1} with a relative intensity of 1.30 (a.u.). Bulk WS_2 Raman spectra show E^1_{2g} band at $\sim$ 351 cm^{-1} and A_{1g} band at $\sim$ 420 cm^{-1}, but in the case of monolayer WS_2 samples, a red-shift occurs for A_{1g} line ($\sim$ 3 cm^{-1}) and a minor blue-shift occurs for the 2LA(M) line (less than $\sim$ 1 cm^{-1}) [9], a behavior clearly observed in Figure 2. For these reasons we concluded that both WS2-S1 and WS2-S2 are monolayer or few layers WS_2 samples.

2 Experimental methods

2.1 THz time domain spectroscopy (THz-TDS)

THz-TDS is a testing method based on a coherent detection, implementing a phase-sensitive technique that enables a large range of application in fields like medicine, chemistry or engineering [10]. In this study, this technique is used to make measurements of material properties at THz frequencies with a spectral range between 0.2 THz and 2 THz. Our system is based on a commercial THz spectrophotometer (TERA K8 of Menlo Systems) with an excitation laser line of 780 nm. The system is working in a transmission setup (see **Figure 3**) because target conducting samples are very thin (less than 10 nm), deposited on a dielectric substrate, so most of the electromagnetic field reaches the emitting antenna. In case of measuring bulk materials (much thicker than the skin depth), a reflection setup could be more adequate.
Figure 3 shows a simplified THz-TDS schema where we can see both optical and THz paths. On the first stage, an optical pulse is generated by the 780 nm laser (blue dashed line). The optical pulse is split by using a polarizing beam splitter into a detecting (red dashed line) and a generating beam (green dashed line). The pump (generating) beam travels along to a fixed length path until it arrives to the emitting THz antenna. The probe (detecting) beam travels along to a variable length path using a controlled delay line until it arrives to the receiving THz antenna. When a pump pulse reaches the emitting antenna, a THz wave is generated and transmitted through the sample. Two collimating lenses are used to reduce the spot size on the sample and a controlled multi-axis system is used in order to align the sample with the spot. When a probe pulse reaches the receiving antenna, a photocurrent, which is proportional to

the instantaneous electric field, is generated and recorded by the acquisition data system. The variable delay line stage allows measuring the different instants of the THz pulse in the temporal domain. After a Fourier transform we obtain the spectra, as the electric field versus frequency.
THz-TDS applied to 2D material measurement consists on, at least, a set of three measurements (see **Figure 4**). The first measurement is used for the characterization of the reference pulse generated by the emitting antena when it travels along the THz path without the presence of the sample or the substrate. Then, the reference signal shown in Equation 1 is the result on the frequency domain of the convolution of the THz pulse in the temporal domain and $h_0(t)$, the impulse response of the THz path channel (air). The second measurement is used to characterize the dielectric properties of the bare substrate by replacing a portion of the previous air path with a new path including the substrate. Then, the substrate signal shown in Equation 2 is the result on the frequency domain of the convolution of the THz pulse in the temporal domain and $h_{sub}(t)$, the impulse response of the THz path channel modified by the substrate contribution. Finally, the third measurement is used to analyze the variations produced by the whole sample in relation to the reference signal. The sample signal shown in Equation 3 is the result on the frequency domain of the convolution of the THz pulse in the temporal domain and $h_{2D}(t)$, the impulse response of the THz path channel modified by the sample contribution (where $\omega = 2\pi f$ is the angular frequency).

$$S_0(w) = H_0(w) \cdot E_0(w) \tag{1}$$

$$S_{sub}(w) = H_{sub}(w) \cdot E_0(w) \tag{2}$$

$$S_{2D}(w) = H_{2D}(w) \cdot E_0(w) \tag{3}$$

The amplitude $\rho_{sub}(w)$ and the phase $\Phi_{sub}(w)$ of the ratio between the substrate signal and the reference signal in the frequency domain, $\mathbb{T}_{sub}(w)$, allows to obtain the dielectric properties of the substrate: $n_{sub}(w)$, the refractive index of the substrate (Equation 5), and $\kappa_{sub}(w)$, the extinction index of the substrate (Equation 6) [11].

$$\mathbb{T}_{sub}(w) = \frac{S_{sub}(w)}{S_0(w)} = \frac{H_{sub}(w)}{H_0(w)} = \rho_{sub}(w) \cdot e^{-i\Phi_{sub}(w)} \tag{4}$$

$$n_{sub}(w) = \Phi_{sub}(w) \cdot \frac{c}{w\, d_{sub}} + 1 \tag{5}$$

$$\kappa_{sub}(w) = \ln\left(\frac{4n_{sub}}{\rho_{sub}(w)(n_{sub}+1)^2}\right) \cdot \frac{c}{w\, d_{sub}} \tag{6}$$

where d_{sub} is the subtrate thickness.
The ratio between the sample signal and the reference signal in the frequency domain, $\mathbb{T}_{2D}(w)$, depends on the dielectric properties of the substrate, which were previously obtained from Equation 5 and 6, and on the properties of the 2D sample. Assuming that the 2D material is a boundary condition of the substrate with a surface conductivity σ_{2D}, the expression could be reduced to Equation 7.

$$\mathbb{T}_{2D}(w) = \frac{S_{2D}(w)}{S_0(w)} = \frac{4Xn_{sub}}{n_{sub}+1} \cdot e^{-i\frac{(\tilde{n}_{sub}-1)\, w\, d_{sub}}{c}} \cdot \sum_{m=0}^{FP} fp_{bound}^{m} \tag{7}$$

$$fp_{bound}(w) = \frac{n_{sub}-1}{n_{sub}+1} \cdot (2n_{sub}X - 1) \cdot e^{-2i\frac{\tilde{n}_{sub}\, w\, d_{sub}}{c}} \tag{8}$$

$$X^{-1} = 1 + n_{sub} + \sigma_{2D} Z_0 \tag{9}$$

where $\tilde{n}_{sub} = n_{sub} - i\kappa_{sub}$ is the complex refractive index of the substrate, $Z_0 = 120\pi\,\Omega$ is the free-space impedance and the FP value of the summation denotes the number of Fabry-Pérot reflections, fp_{bound}, produced in the substrate.
A proper waveform truncation fixes the value of FP: for thick substrates and short time windows, the summation could be equal to 1 leading to Equation 10, considering only the first pulse [12]. For thin substrates and long time windows, the summation could be approximated to a simplified expression (see Equation 11) after considering infinite internal reflections [1]. For intermediate situations, the FP value could not be exactly an integer (depending on the time window used), so the resulting expression can not be analytically calculated and, even using numerical analysis, the result could not properly fit the Fabry-Pérot effect.

$$\sigma_{2D} = \frac{1}{Z_0}\left(\frac{4n_{sub}}{\mathbb{T}_{2D}(w)\cdot(n_{sub}+1)}\cdot e^{-i\frac{(\tilde{n}_{sub}-1)\,w\,d_{sub}}{c}} - 1 - n_{sub}\right) \tag{10}$$

For this reason, instead of using Equation 7, we can use simplified expressions depending on the thickness of the substrate. If the substrate is thin, a large time window could be used for processing the data and the conductivity may be calculated numerically from Equation 11 (and the definitions on Equation 8 and 9). On the other hand, if the substrate is thick enough, a truncated time window including only the first pulse could be used and then the conductivity could be calculated from Equation 10.

$$\mathbb{T}_{2D}(w) = \frac{4Xn_{sub}}{n_{sub}+1}\cdot e^{-i\frac{(\tilde{n}_{sub}-1)\,w\,d_{sub}}{c}}\cdot\frac{1}{1-fp_{bound}} \tag{11}$$

The criterion of the thickness of the substrate and, for extension, the time window used is not absolute and it depends on the dielectric properties of the substrate, i.e. the speed of the wave in the medium.

2.2 Rutile dielectric resonator (RDR)

The conductivity of a conducting sample can also be obtained from the quality factor, Q, changes on a dielectric resonator cavity at the microwave range of frequencies. This method allows obtaining the electrical resistance of the material on a single frequency (the resonance frequency of the cavity) depending on the dielectric properties of the materials involved and on the cavity size [2].
The cavity used in our measurements was a closed metallic body with a rutile (TiO2) cylinder of 3 mm height and 4 mm diameter shielded axially by a pair of square samples of approximately 12 mm side. Samples were fixed with a pair of bulk brass blocks and the electromagnetic field was generated by a pair of coaxial cables with coupling loops at the end (see **Figure 5**) [2, 13].
The experimental process consists on measuring the spectrum of the S_{21} parameter with a vector network analyzer in order to obtain the resonance frequency, f_0, and the quality factor, Q, of the resonator. The resonance mode used was the TE_{011} mode and f_0 varies from 8.5 to 9.5 GHz. The value of f_0 depends on the physical dimensions of the cavity (3 mm height), the dielectric constant of the rutile ($\epsilon_r \sim 100$) and, in a minor way, the skin depth of the target sample, δ_s, which is a measure of how close to the surface the electrical current flows, at certain frequency, f (see Equation 12).

$$\delta_s = \sqrt{\frac{\rho}{\pi\cdot f\cdot\mu_0}} \tag{12}$$

where $\mu_0 = 4\pi\times10^{-7}\,\mathrm{H\ m^{-1}}$ is the permeability in vacuum and ρ is the resistivity of the material.
The skin depth also introduces a relation between the surface resistance, R_S, and the resistivity, ρ (see Equation 13).

$$R_S = \frac{\rho}{\delta_s} \tag{13}$$

The quality factor of the resonator is a measure of the ratio between the energy stored and the energy dissipated by the resonator and could be obtained from S_{21} spectrum by dividing the resonance frequency by the bandwidth at 3 dB. Equation 14 shows the relation between the surface resistance of the surfaces enclosing the cavity (the sample) and the quality factor of the resonator [2].

$$\frac{1}{Q} = \sum_i \frac{R_{S_i}}{R_{GS}} + p \cdot \tan(\delta) \tag{14}$$

where the sum considers the losses of the individual metal surfaces noted through the index i, $R_{GS} = 242.529\,\Omega$ is the geometrical factor of the closing plates of the resonator, $p \sim 1$ is the ratio of the energy stored in the rutile to the energy stored in the entire resonator, $\tan(\delta) = 1.2496 \times 10^{-4}$ is the loss tangent of rutile at room temperature. Note that the lateral walls can be neglected because the small size of the rutile cylinder (compared with the total size of the cavity) ensures that the electromagnetic field in the walls are effectively zero.
The resistivity of the samples, ρ, could be obtained from the definition of the skin depth (Equation 12), the relation between the skin depth and the surface resistance (Equation 13) and the value of R_S obtained experimentally from Equation 14 at the resonance frequency, f_0, as shown in Equation 15.

$$\rho = \frac{{R_S}^2}{\pi \cdot f_0 \cdot \mu_0} \tag{15}$$

3 Experimental results

3.1 THz-TDS results

Time domain electric field amplitude provided by THz-TDS on WS_2 samples shows the influence of the WS_2 layer in terms of pulse attenuation and delay (see **Figure 6**). The main reference pulse (green signal) is reduced by 16.2 % when it goes through the bare substrate (blue signal) and it is reduced by 26.3 % when it passes through the WS_2 sample (red signal), so the relative attenuation introduced by the WS_2 layer is approximately 12 %. Quartz substrate 1 mm thick produces a delay of 3.1 ps from reference (air) and an the WS_2 layer produces an extra delay of 0.1 ps. The blue minor peak at 18.30 ps represents the first Fabry-Pérot reflection and provides a metric for selecting the time window. The distance between the first blue pulse (at 5.73 ps) and the secondary pulse (at 18.30 ps), about 12.57 ps, also provides an estimation for the refractive index of the substrate ($n_{sub} \sim 1.81$) based on the wave speed reduction from the free-space value (going twice through the thickness of the sample).
The attenuation affects all the frequencies as shown on the spectrum of **Figure 7**, obtained by applying the FFT on the time-domain signal. Dielectric properties of quartz, n_{sub} and κ_{sub}, were obtained from reference and bare substrate spectra ratio, $\mathbb{T}_{sub}(w)$, the value obtained for the refractive index was constant over the frequency range (see **Figure 8**) and very close to the estimation: $n_{sub} \sim 1.847$. Figure 8 also shows the values obtained for the other substrates: $n_{sub} \sim 2.144$ for Quartz-Gr and $n_{sub} \sim 1.713$ for PET-Gr.
From reference and sample spectra ratio, $\mathbb{T}_{2D}(w)$, and applying the model of infinite Fabry-Pérot reflections of Equation 11 (after using a proper time window), the sheet conductivity obtained is shown on **Figure 9** (blue curve on line). For comparison, on the same Figure 9 we reported the conductivity values obtained for other 2D materials: MoS_2 on sapphire [1] and graphene on Quartz (Gr-Quartz). The conductivity obtained for WS_2 on Quartz was in the range between 1 and 3 mS/□, slightly higher to that obtained for graphene on Quartz (between 0.5 and 1 mS/□).
In case of GrO and Gr-flakes samples, time domain analysis shows that the THz-TDS method in the transmission setup is not adequate for these materials.It could be due to the roughness and non uniformity of the samples. Moreover, since graphene oxide is an insulator, GrO sample is practically invisible to the electromagnetic field and the thickness is not enough to apply the bulk material approximation

(the same used to characterize the bare substrates). For the reduced graphene oxide, it is a good conductor and the thickness of Gr-flakes sample is large enough to avoid transmitting the terahertz pulse, so the receiving antenna does not receive the signal.

3.2 RDR results

The experimental results obtained by this method are summarized in **Table 2**. As a calibration, the first measurement done on the RDR was an empty setup (without samples) with a very low coupling. The resonance frequency obtained in this preliminary measurement was 9.0262 GHz and the quality factor was 1742. The resistivity obtained for these values was $\rho = 8.32 \cdot 10^{-2}\,\mu\Omega\,\mathrm{m}$ which is in good agreement with the values found in the literature for bulk brass $\sim 6 \cdot 10^{-2}$ - $9 \cdot 10^{-2}\,\mu\Omega\,\mathrm{m}$. For a copper sample of 1 mm thickness we obtained a resistivity value of $\rho = 1.70 \cdot 10^{-2}\,\mu\Omega\,\mathrm{m}$ which is also in good agreement with the value found in the literature for bulk copper $\sim 1.72 \cdot 10^{-2}\,\mu\Omega\,\mathrm{m}$. The frequency shift in these previous measurements was very small, about 12.7 MHz, and it corresponded only with the difference between the skin depth of each material because the geometry of the cavity was basically the same.
The values found for graphene on PET (Gr-PET) and graphene on quartz (Gr-Quartz) samples were very different. Both samples producing a higher shift on the resonance frequency (between 500 and 900 MHz lower) which is due to a drastic change in the geometry of the cavity (larger cavity due to the substrate thickness). The conclusion is (as in the other method), these 2D samples are too thin and therefore cannot shield the electromagnetic field properly. Furthermore, the Q values obtained were also too low and the noise level too high to extract reasonable values for the surface resistance.
In case of GrO samples, as found in THz-TDS method, the material was invisible. The configuration used was copper-sample-rutile-sample-copper and the values obtained were basically the same as found in the previous measurement with only copper. This was not a surprising result because the GrO is an insulator. The minor differences in the frequency and the quality factor obtained respect the only copper configuration is due to the geometric change by addition of the layer.
Finally, in the case of Gr-flakes samples, the value of the resonance frequency obtained was identical to that of the configuration with only copper, while the quality factor decreased dramatically from 3052 to 878.0. With these data, the resistivity obtained was $\rho = 1.37\,\mu\Omega\,\mathrm{m}$ which corresponds to a surface conductivity of $4.5\,\mathrm{S}/\square$ and a skin depth of $6.2\,\mu$m (slightly larger than the thickness of the sample). This value is reasonable compared with the value obtained for Gr-Quartz from THz-TDS as the surface conductivity is 4 500 times greater when the thickness relation of the samples is in the same order of magnitude (between 2 500 and 6 000 considering $\sim$ 3 - 7 graphene layers).

4 Comparison and conclusions

4.1 Comparison

Both THz-TDS and RDR are contactless and non-destructive measuring methods for obtaining the conductivity of thin metallic samples. However, there are several differences between both methods.
They are complementary in terms of frequency ranges because dielectric resonators work on microwave range (few GHz) and THz-TDS work from hundreds of GHz up to 2 THz. Nevertheless, THZ-TDS method is more suitable since it allows obtaining a wide spectrum (from 0.2 GHz to 2 THz) while RDR only allows obtaining the conductivity for a single frequency.
In terms of sample size, THz-TDS method has no important limitations but is better to have big samples (at least 10 mm side) in order to ensure that all the electromagnetic field passes only through the sample. Thus, for small samples compared with the spot size, is mandatory that the lenses are perfectly aligned in the center of the sample. In case of RDR method, the size is fixed at 12 mm side (in fact, a little less) in order to fit the cavity, so bigger samples cannot be measured. Smaller samples can be measured because the rutile cylinder diameter is 4 mm only but, in this case, the alignment complexity increases and the quality of the results obtained decreases. For these reasons, the RDR method has more sample size limitations.

The transmission setup used in the THz-TDS method is very adequate for thin samples (which is the case of 2D material) because the major part of the electromagnetic field reaches the receiving antenna. In case of RDR method, the electromagnetic field should be confined in the cavity in order to produce the resonance between the samples surfaces for this reason the minimum thickness required is between 2 and 3 times the skin depth of the target material. For these reasons, in terms of samples thickness, the methods are opposite.
The time spent in data acquisition and data processing is lower in case of RDR method. THz-TDS method requires models and algorithms more complex and the calibration time is also longer.
Despite it is possible to measure with a unique sample, as shown in [13], RDR method needs two identical samples in order to obtain the best results (using only one sample increase the error sources and needs more measurement stages). THz-TDS method requires only one sample of the 2D material but a sample with a bare substrate is also needed and the minimum number of measurements required is 3, in comparison with RDR method which only need a unique measurement in case of samples with enough thickness.

4.2 Conclusions

The samples used in each method, THz-TDS or RDR, could not be the same, as the restrictions for each experiment setup are different:

- For RDR in our actual setup we need 12 × 12 mm square samples with thickness greater than the skin depth.
- For THz-TDS in a transmission setup the samples could be monolayers. They have to be flat and uniform, over the laser spot size surface.

We used THz-TDS on CVD obtained WS_2 samples, obtaining the electrical sheet conductivity up to 2 THz. The conductivity is high, between 1 and 3 mS/□, very close to the values obtained for graphene or MoS_2.

Supporting Information
Supporting Information is available from the Wiley Online Library or from the author.

Acknowledgements
The authors wish to thank the Scientific and Technological center, Universitat de Barcelona (CCiT-UB) services for Raman spectroscopy facilities, the prof. J. Eom from Sejong University, Korea, for WS_2 samples, and D. Gabriel for his help in the laboratory and revision of the algorithms. The authors also wish thank Danubia NanoTech Ltd. for samples of graphene oxide and reduced graphene flakes and V. Skákalová for her interesting comments.

References
1 D. Arcos, D. Gabriel, D. Dumcenkco, A. Kis, N. Ferrer-Anglada, Phys. Status Solidi B 2016. DOI 10.1002/pss
2 P. Krkotić, A. Aguasca and J. M. O'Callaghan, 48th European Microwave Conference (EuMC), Madrid, 2018. DOI: 10.23919/EuMC.2018.8541442.
3 J. H. Choi, J. Lee, M. Byeon, T. E. Hong, H. Park, C. Y. Lee ACS Applied Nano Materials 2020, 3, 3, 2257-2265 DOI: 10.1021/acsanm.9b02378
4 X. Zhang, L. Hou, A. Ciesielski, P. Samorì, Adv. Energy Mater. 2016, 6(23), 1600671. ISO 690
5 M. Bozzi, L. Pierantoni, S. Bellucci, Radioengineering 2015, 24, 3, 661.
6 Z. Sun, A. Martinez, F. Wang, Nat. Photonics 2016, 10, 4, 227-238.
7 Q.H. Wang, K. Kalantar-Zadeh, A. Kis, J.N. Coleman, M.S. Strano, Nat. Nanotechnol. 2012, 7, 699-712.
8 F. Wang, I.A. Kinloch, D. Wolverson, R. Tenne, A. Zak, E. O'Connell, U. Bangert, R. J. Young, 2D Mater. 2016, 4.
9 T. A. Loh, D. H. Chua, A. T. Wee, Sci. Rep. 2015. 5, 18116.
10 J. Neu, C. A. Schmuttenmaer, J. Appl. Phys. 2018, 124, 23, 231101.

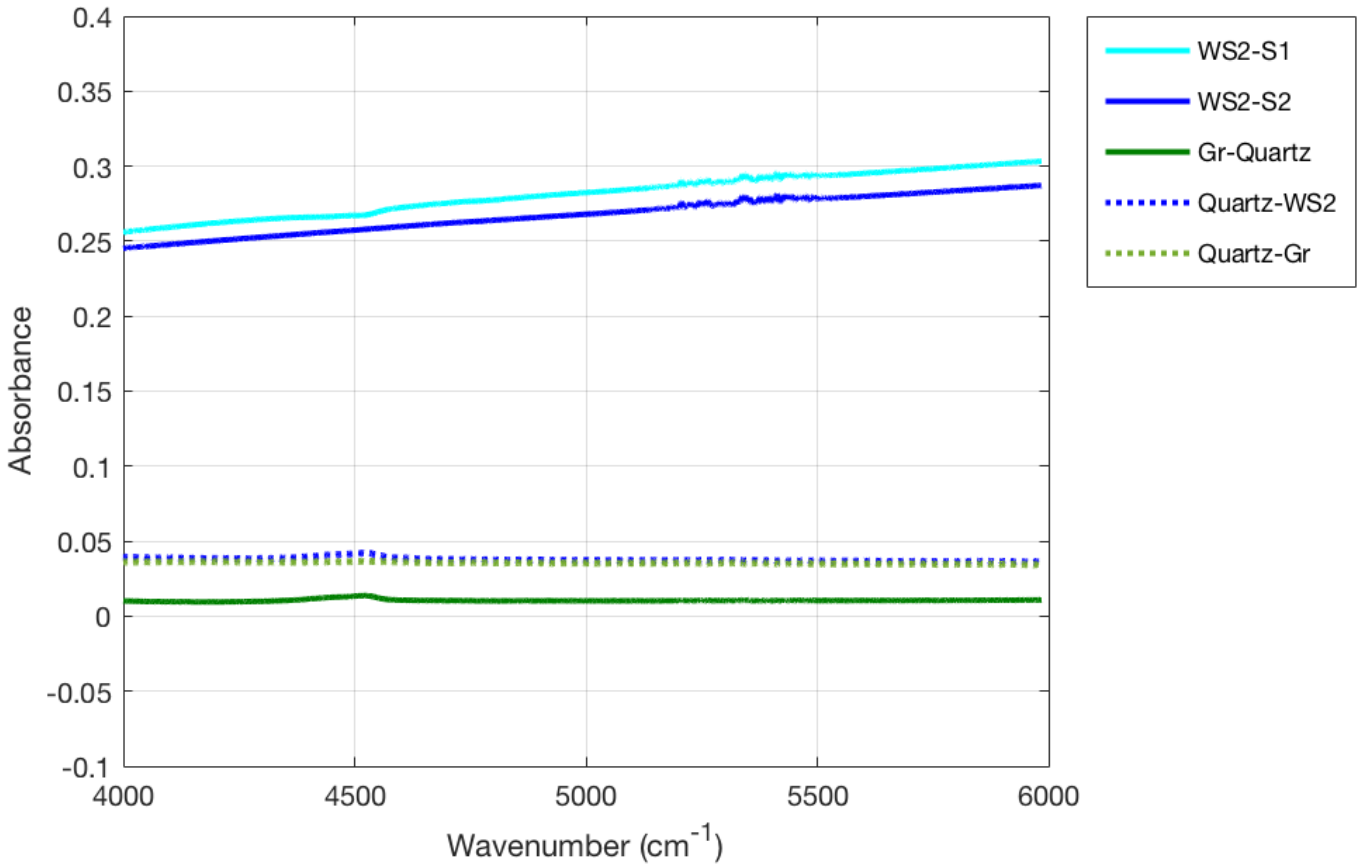

Figure 1: IR absorbance of WS_2, graphene and quartz substrates.

11 Y. S. Jin, G. J. Kim, S. G. Jeon, J. Korean Phys. Soc. 2006, 49, 2, 513-517.
12 M. Liang, Z. Wu, L. Chen, Li. Song, P. Ajayan, H. Xin, IEEE Transactions on Microwave Theory and Techniques 2011, 59, 10, 2719-2725.
13 D. Arcos, P. Krkotić, J. O'Callaghan, M. Pons, L. Ametller, N. Ferrer-Anglada, Phys. Status Solidi B 2019.

Table 1: Llist of analyzed samples.

Material	Substrate	Notation	Area [mm × mm]	Thickness [mm]
WS_2	Quartz	WS2-S1	20×20	-
WS_2	Quartz	WS2-S2	20×20	-
Quartz	-	Quartz-WS2	20×20	$1.0 \pm 5\%$
Graphene	PET	Gr-PET	11.8×11.8	-
PET	-	PET-Gr	11.8×11.8	$0.25 \pm 5\%$
Graphene	Quartz	Gr-Quartz	11.8×11.8	-
Quartz	-	Quartz-Gr	11.8×11.8	$0.50 \pm 5\%$
Graphene Oxide	-	GrO	11.8×11.8	$(13 \pm 1) \cdot 10^{-3}$
Reduced Graphene Oxide	-	Gr-flakes	11.8×11.8	$(10 \pm 1) \cdot 10^{-3}$

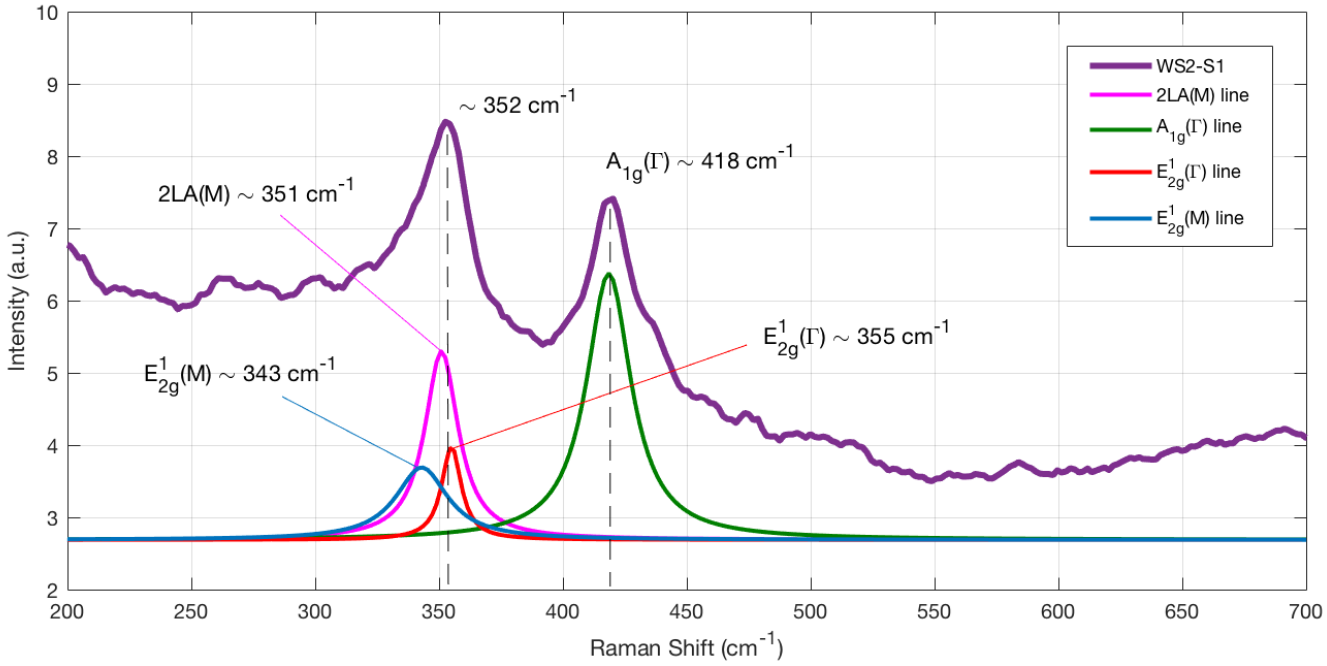

Figure 2: Raman spectra of WS2-S1 sample (WS_2 on quartz) and multi-peak Lorentzian fitting of Raman bands shows the two lines $E^1_{2g}(\Gamma)$ at 355 cm^{-1} and $A_{1g}(\Gamma)$ at 418 cm^{-1} characteristics of monolayer or few layers [8, 9].

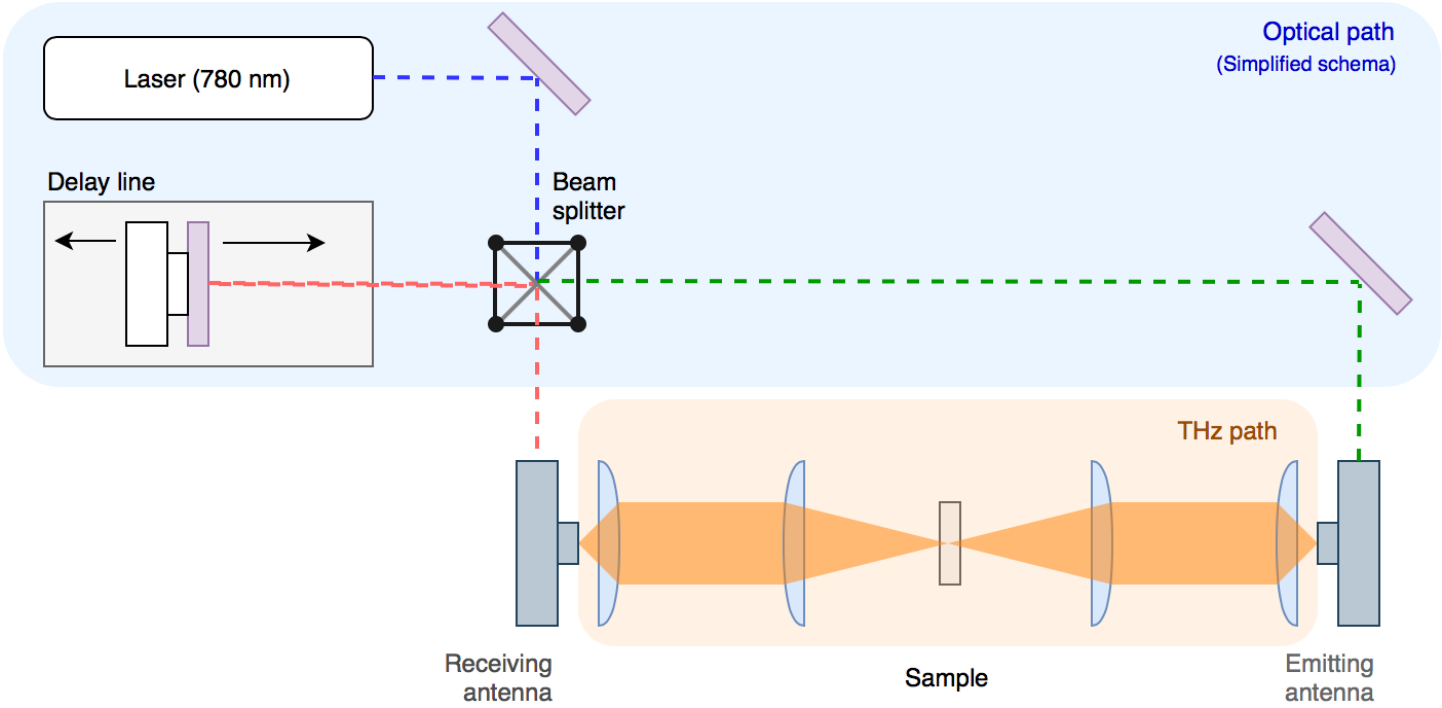

Figure 3: THz-TDS schema of the transmission setup based on a commercial THz spectrophotometer TERA K8.

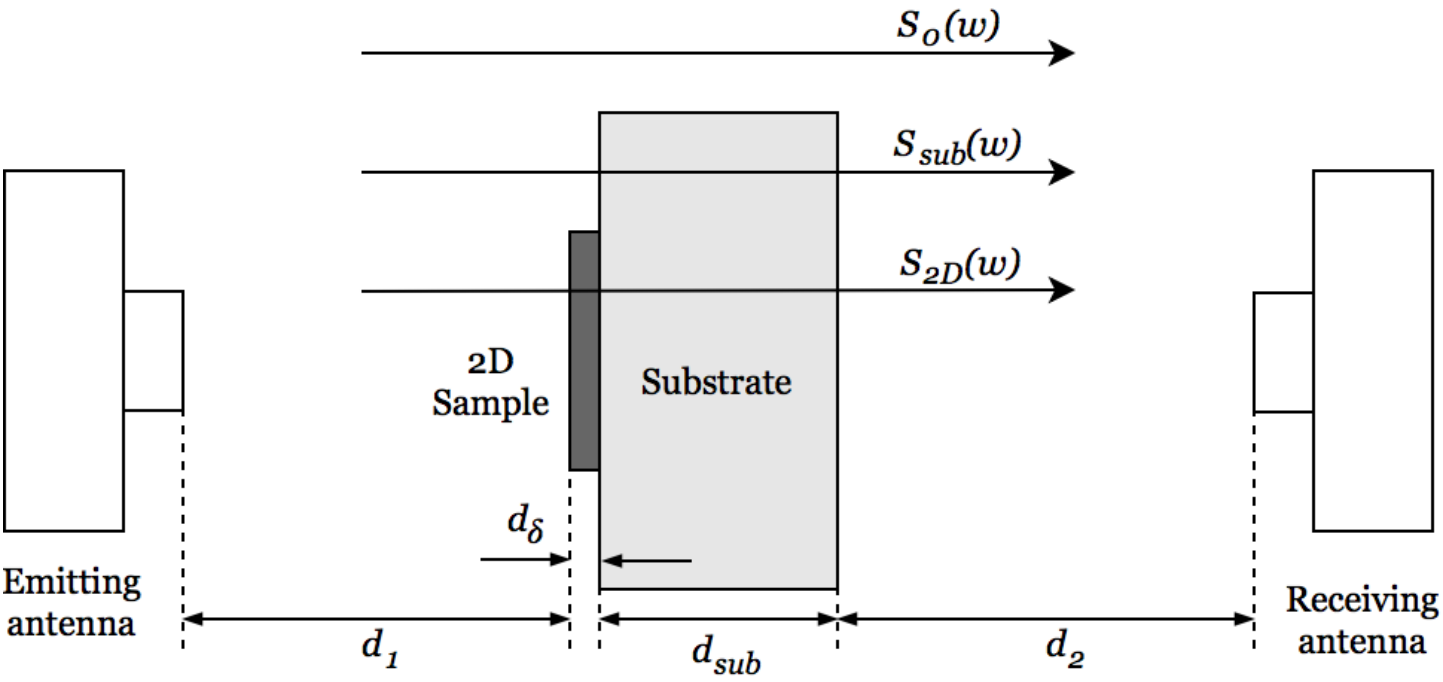

Figure 4: Optical diagram of the THz beams between the transmitting and receiving antennas.

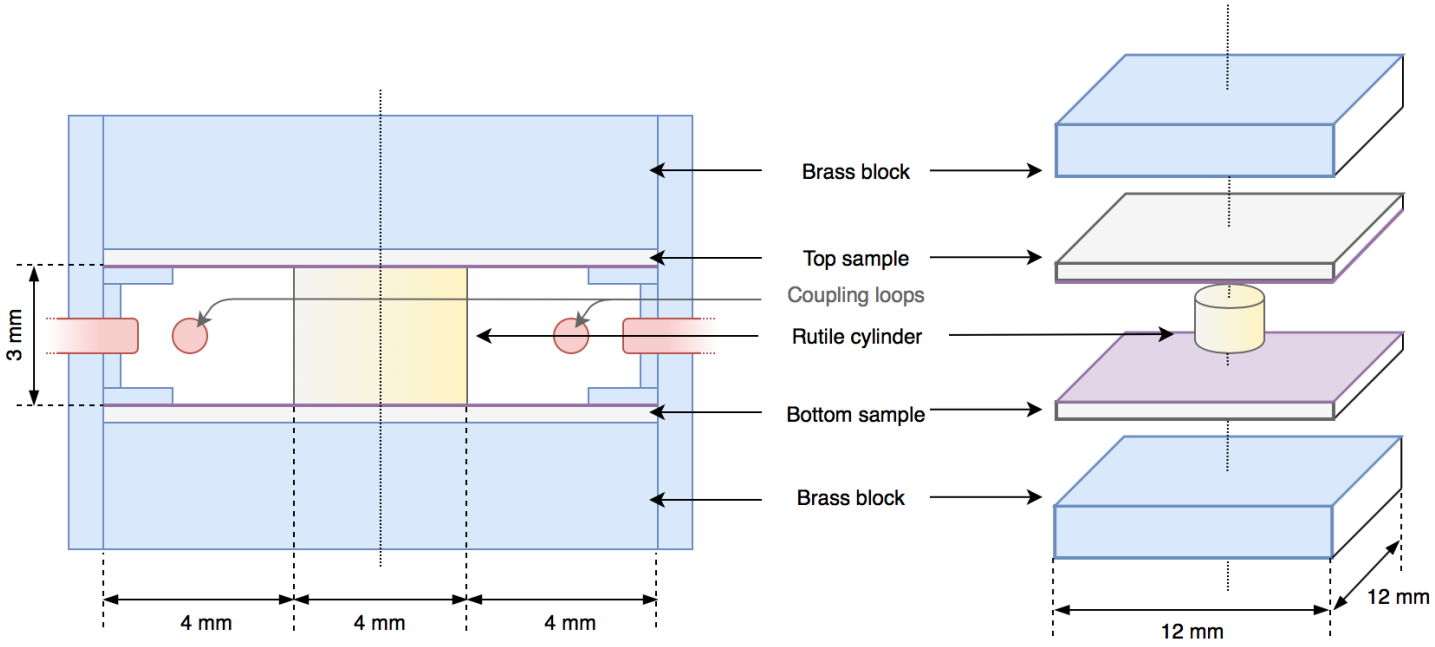

Figure 5: Scheme of the RDR cross-section and the inner layers.

Table 2: Summary of the resonance frequency f_0, the quality factor Q, the surface resistance R_S, and the resistivity ρ obtained for Brass, copper and the graphene-based samples.

Sample	f_0 [GHz]	Q	R_S [mΩ]	ρ [$\mu\Omega$ m]
Brass	9.0262	1742	54.5	$8.32 \cdot 10^{-2}$
Copper	9.0135	3052	24.6	$1.70 \cdot 10^{-2}$
Gr-PET	8.4834	417	-	-
Gr-Quartz	8.1243	154	-	-
GrO	9.0075	3006	-	-
Gr-flakes	9.0135	878.0	221	1.37

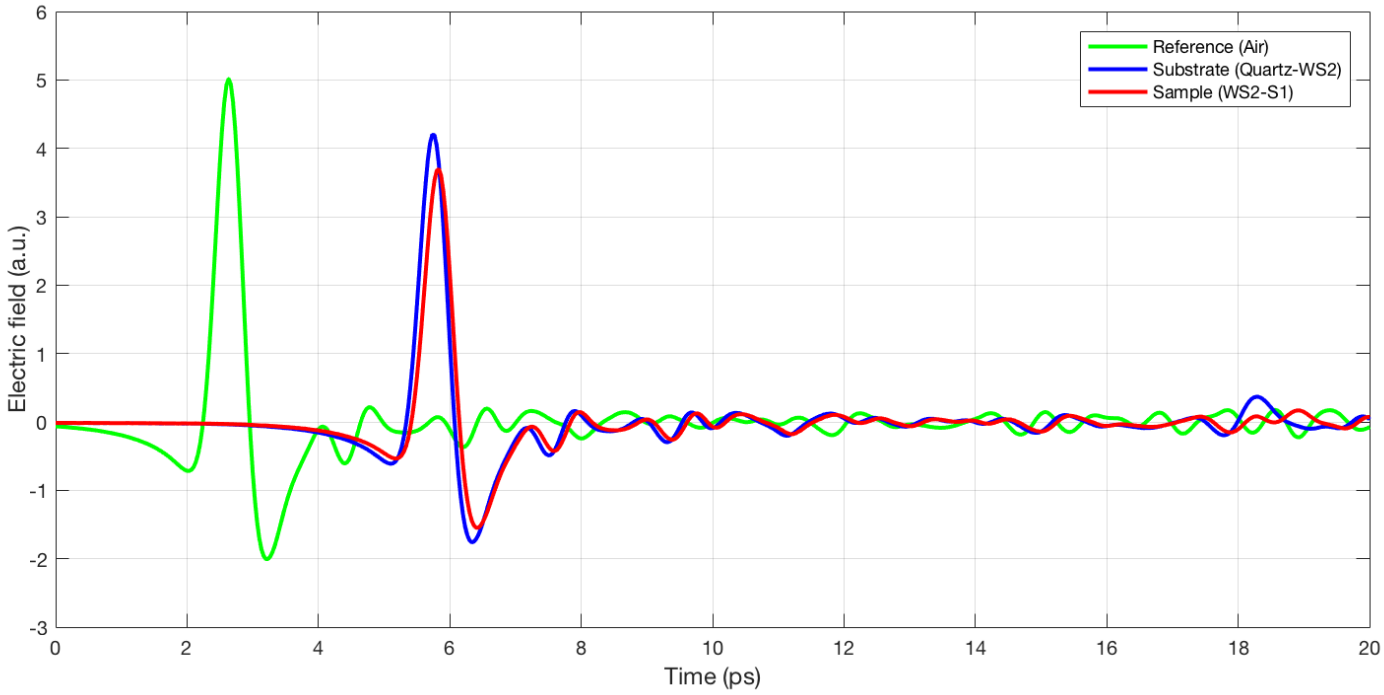

Figure 6: Time-domain electric field pulse of the transmitted THz wave through the reference (air), the bare substrate (quartz) and the WS_2 sample on the substrate.

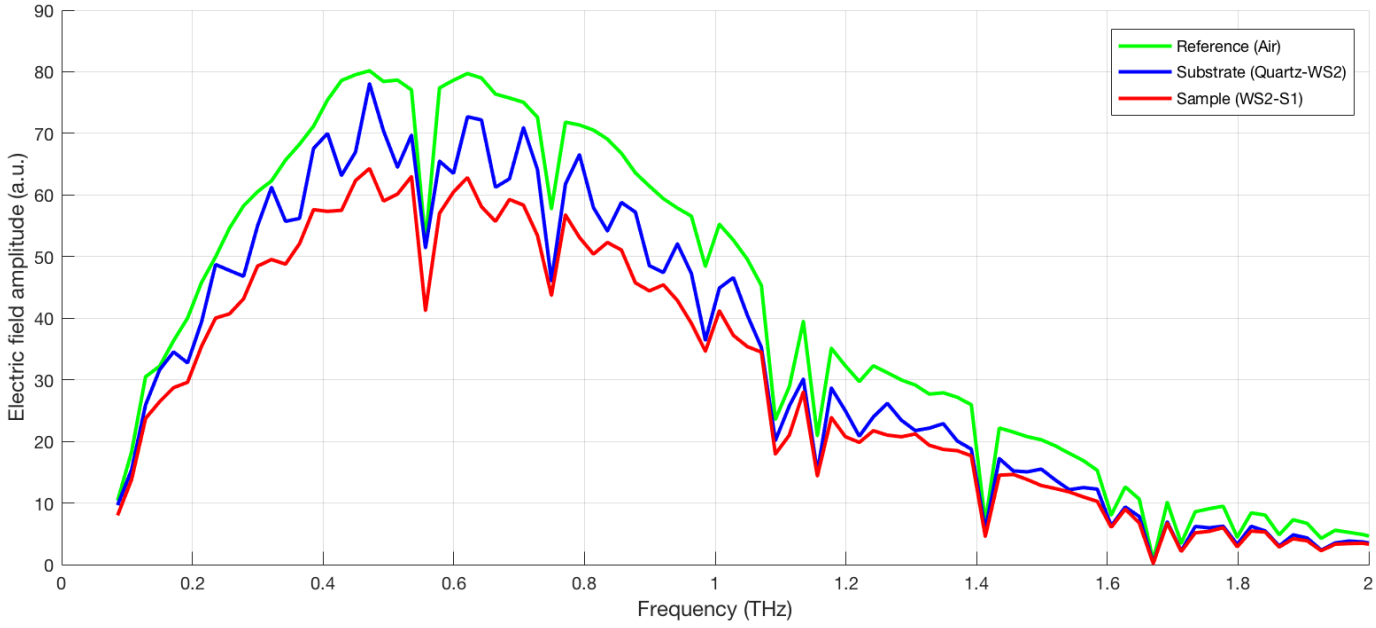

Figure 7: Electric field amplitude spectra of the reference (air), the bare substrate (quartz) and the WS_2 sample on the substrate

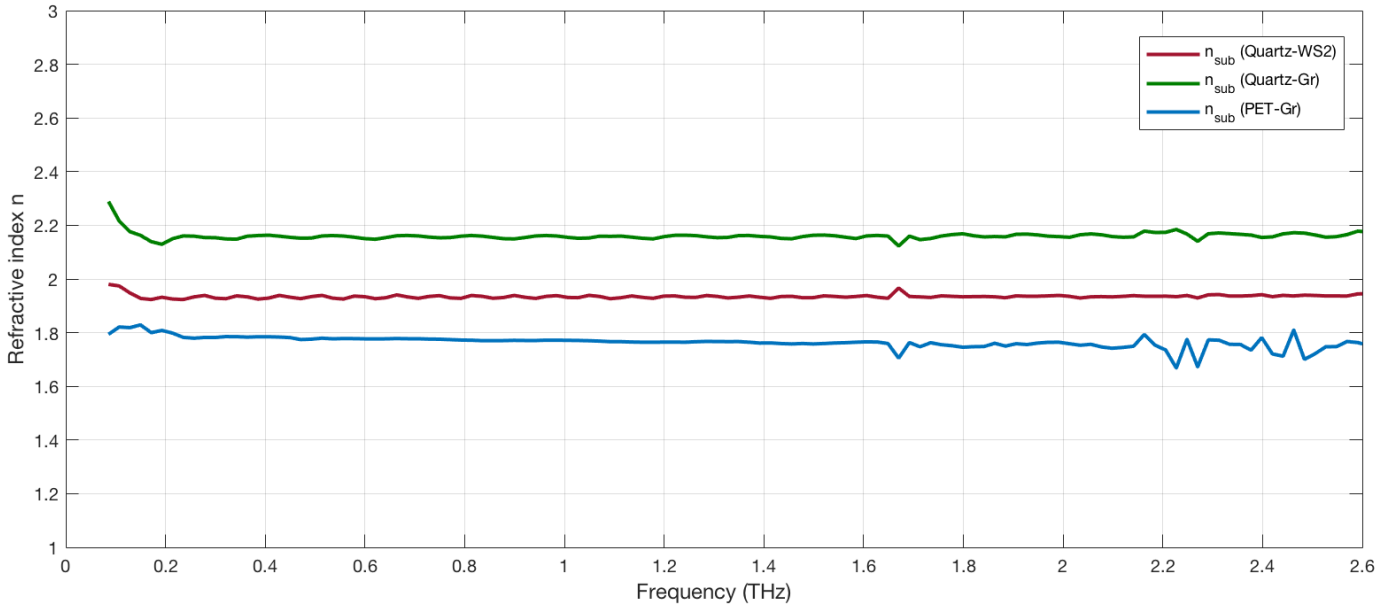

Figure 8: Refractive index of the substates (Quartz-WS2, Quartz-Gr and PET-Gr).

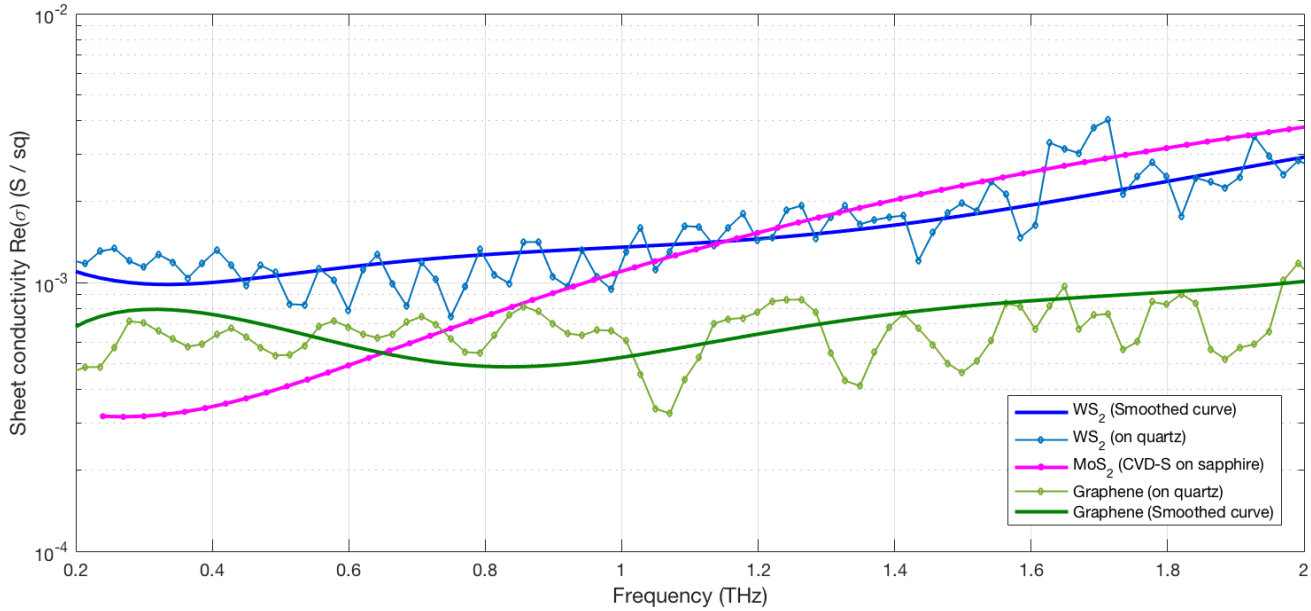

Figure 9: Real part of sheet conductivity of WS_2 (WS2-S1), graphene (Gr-Quartz), and MoS_2 [1].